JACS
JOURNAL OF THE AMERICAN CHEMICAL SOCIETY
Article
pubs.acs.org/JACS

Large-Scale Hot Spot Engineering for Quantitative SERS at the Single-Molecule Scale

Hung-Ying Chen,*[,†] Meng-Hsien Lin,[†] Chun-Yuan Wang,[†] Yu-Ming Chang,[‡] and Shangjr Gwo*[,†,§]

[†]Department of Physics, National Tsing-Hua University, Hsinchu 30013, Taiwan
[‡]Center for Condensed Matter Sciences, National Taiwan University, Taipei 10617, Taiwan
[§]National Synchrotron Radiation Research Center, Hsinchu 30076, Taiwan

Supporting Information

ABSTRACT: Quantitative surface enhanced Raman spectroscopy (SERS) requires precise control of Raman enhancement factor and detection uniformity across the SERS substrate. Here, we show that alkanethiolate ligand-regulated silver (Ag) nanoparticle films can be used to achieve quantitative SERS measurements down to the single-molecule level. The two-dimensional hexagonal close-packed superlattices of Ag nanoparticles formed in these films allow for SERS detection over a large area with excellent uniformity and high Raman enhancement factor. In particular, the SERS signal from the thiolate ligands on Ag nanoparticle surfaces can be utilized as a stable internal calibration standard for reproducible quantitative measurements. We demonstrate the capability of quantitative SERS by measuring the areal densities of crystal violet molecules embedded in an ultrathin spin-on-glass detection "hot zone", which is a planar and uniformly enhanced region several nanometers above the Ag nanoparticles. The Raman measurement results exhibit a linear response over a wide dynamic range of analyte concentration.

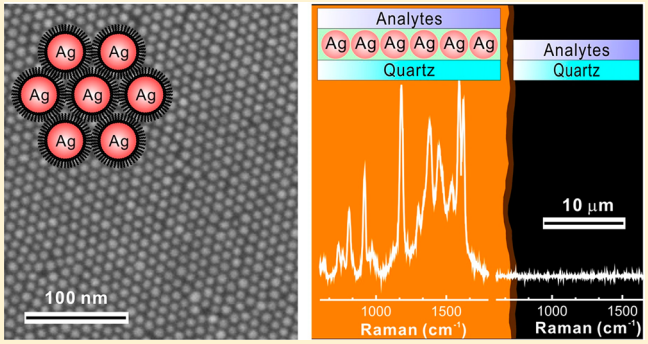

INTRODUCTION

Raman spectroscopy arises from the inelastic light scattering by molecular vibrations, which could provide "fingerprint" information for molecular diagnostics. However, the inherently low scattering intensity of conventional Raman spectroscopy limits its widespread applicability. Over the last few decades, surface enhanced Raman spectroscopy (SERS)[1−4] has received intense attention because of its great potential for ultrasensitive detection down to the single-molecular level.[5−9] In SERS, light excitation of surface plasmon resonances in noble-metal nanostructures significantly enhance and localize the incident electromagnetic field at nanoscale "hot spots". The Raman intensity of molecules, which are placed in close proximity to the hot spots of SERS substrate, can be dramatically amplified with an enhancement factor frequently above 10^6.[10−12]

However, due to the random distribution of hot spots on the SERS substrate, only part of the analytes can be really accounted for. For this reason, although it is obvious that the precise determination of analyte concentration is critical for biological and chemical sensing applications, there are only a few reports focused on the realization of quantitative SERS measurements.[13−15] To realize highly sensitive and reliable SERS for quantitative measurements, there have been numerous attempts to simultaneously achieve large Raman enhancement factor and reproducibility of hot spots using different nanofabrication techniques.[16−21] However, until now, it is still unattainable because of limited uniformity and controllability of hot spots in available SERS substrates.[22−26] Here, we show that alkanethiolate ligand-regulated silver nanoparticle (AgNP) superlattices can be applied to achieve highly enhanced and uniform Raman measurements over a large area (>1 cm^2). The large-scale self-assembly of 6 nm-diameter AgNPs adopted here allows for the formation of regular, close-packed AgNP superlattices, which can function as SERS substrates with excellent uniformity (<5% variation) and large Raman enhancement factor (>1.2 × 10^7). In particular, the SERS signal from the thiolate ligands on the AgNP surface is found to be a robust internal calibration standard for quantitative SERS measurements. Using these substrates, we demonstrate the capability of quantitative SERS detection by measuring the areal density of crystal violet (CV) molecules embedded in a ultrathin (5 nm) spin-on-glass "hot zone", which shows a linear response over a wide dynamic range of CV concentration (5−5000 molecules/μm^2).

There are several major SERS issues need to be addressed to realize quantitative SERS in an efficient and reliable way. First of all, uniform and large SERS substrates are crucial for quantitative measurements. But the required nanofabrication precision to create metal nanostructure arrays with uniform hot spot properties is very difficult to be accomplished.[18,21] Here, we demonstrate that self-assembled AgNP superlattices

Received: August 27, 2015
Published: October 15, 2015

DOI: 10.1021/jacs.5b09111
J. Am. Chem. Soc. 2015, 137, 13698−13705

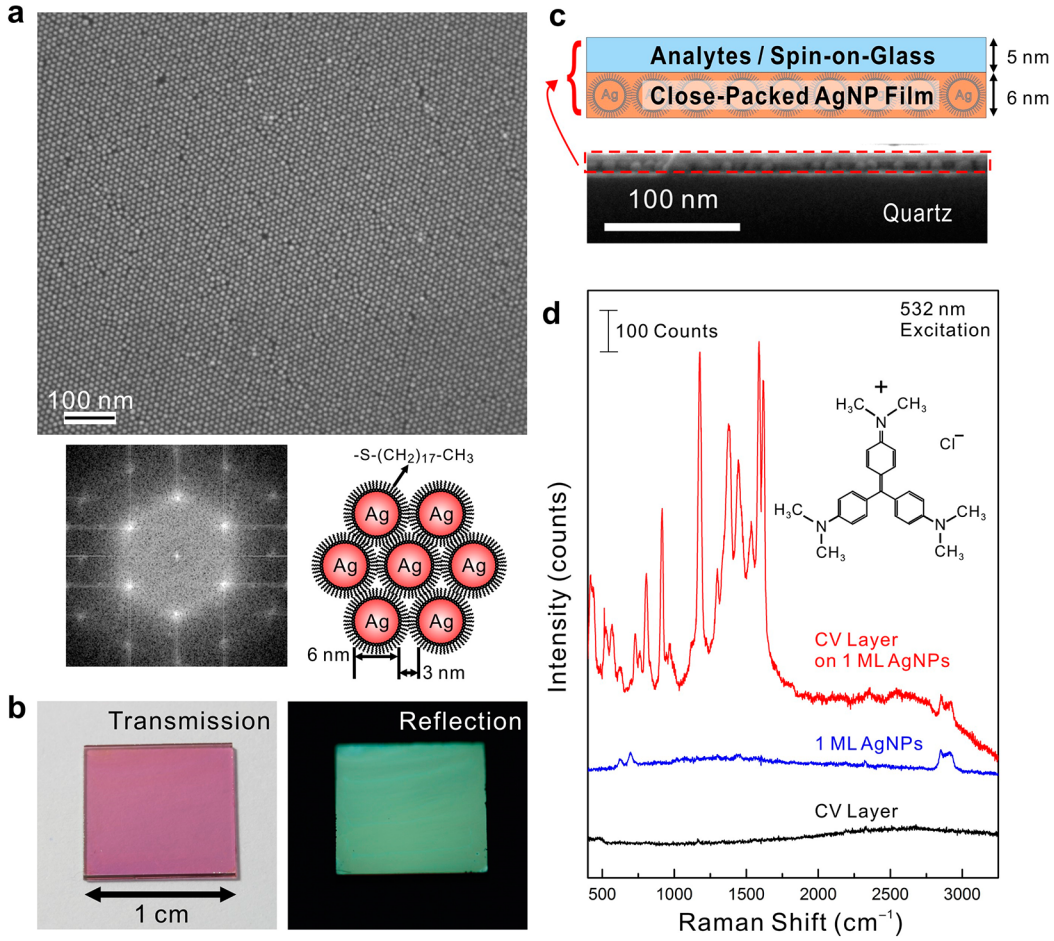

Figure 1. Single-monolayer AgNP film as SERS substrate. (a) Field-emission scanning electron microscopy (FESEM) image of one-monolayer (1 ML) close-packed AgNP film on quartz with an image area of $1 \times 0.7\ \mu m^2$. The diffraction pattern was acquired from fast Fourier transform with an image area of $0.7 \times 0.7\ \mu m^2$. The schematic shows that the interparticle gap is regulated by the thiolate chain length. (b) Transmission and reflection photographs of a large-area ($1 \times 1\ cm^2$), highly uniform 1 ML AgNP film on quartz, illustrating the effect of collective plasmonic resonance. (c) Structure of the SERS substrate (close-packed AgNP film) and the analyte layer, which is a spin-coated layer of crystal violet (CV) molecules embedded in spin-on-glass (SOG). The cross-sectional SEM image shows the thicknesses of CV/SOG layer and AgNP film are about 5 and 6 nm, respectively. (d) Raman spectra (vertically offset for clarity) obtained from a CV/SOG layer on a AgNP film, a bare AgNP film, and a bare CV layer, respectively. The spectra were acquired by using the Raman System I.

regulated by the alkanethiolate surface ligands can resolve this SERS issue. Second, in order to obtain a reproducible SERS signal, subnanometer precise control of the distance between the analyte and the hot spot is necessary because that the SERS signal can be drastically changed even the location of analyte relative to the hot spot is only slightly varied on the nanometer scale.[11,12,27] The advantage of using alkanethiolate surface ligand for nanoparticle self-assembly is that precise interparticle gap control can be achieved by using different alkanethiolate chain length.[28]

In SERS, the overall signal intensity is essentially the sum of signals from all the analytes on the whole detection area covered by the excitation laser beam. In a study by Dlott et al.,[11] it has been shown that the local Raman enhancement factors on Ag-film-on-nanospheres SERS substrate exhibit a broad distribution ranging from 10^4 to 10^{10}. Notably, one-half of the overall SERS signal comes from the hot spots with enhancement factors greater than 10^8, which only account for less than 1% of total hot spots. These findings answer most of the questions about the inhomogeneous nature of the SERS substrates reported in the literature. Over the years, many research efforts have been devoted to optimizing SERS substrates in order to provide the largest magnitude of SERS enhancement. In contrast, the strategy proposed here for reliable quantitative SERS measurements is to avoid anomalously hot detection sites (conventional hot spots), and position analytes in a planar and uniform "hot zone", which is several nanometers above the AgNP film. Meanwhile, the achieved Raman enhancement factor is spatially uniform and sufficiently high ($>10^7$) for single-molecule detection.

The third issue of quantitative SERS concerns about the measurement of absolute SERS signal, which is very difficult to achieve by conventional SERS techniques. The Raman scattering intensity typically depends on various instrumental conditions, rendering it difficult to reproduce the signal even for the same sample. A possible solution for this problem is to establish internal standards,[14,15,29] which might come from the SERS signals of independent and stable components included in the sample. Here, we demonstrate that the SERS signal of passivating alkanethiolate ligands on the AgNP surfaces can be used as a stable internal calibration standard for quantitative SERS measurements.

DOI: 10.1021/jacs.5b09111
J. Am. Chem. Soc. 2015, 137, 13698−13705

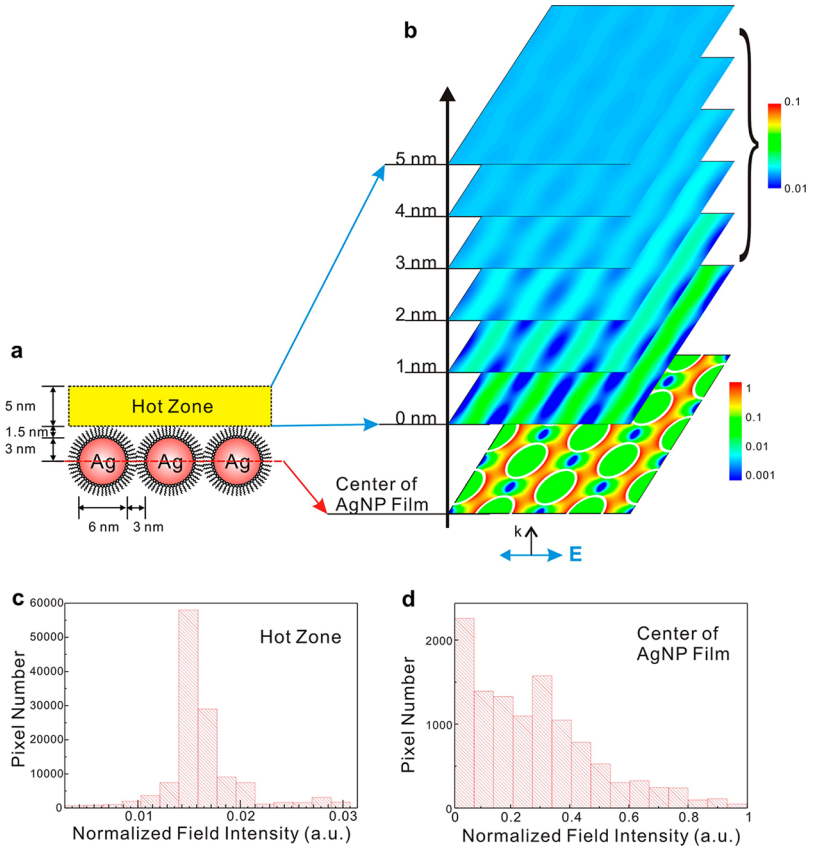

Figure 2. FDTD simulated field distributions. (a) Schematic view illustrating the detection hot zone, where the analytes are located in the controllable region. (b) FDTD simulated electric field intensity ($|E|^2$) distribution at different vertical planes on top of the AgNP film. All the field intensities are normalized to the hottest point in the center plane of the AgNP film. The distribution of hot spots in the center plane of AgNP monolayer film is simulated using a linearly polarized laser at normal incidence. At planes with increasing heights, the features of hot spots become blurred rapidly and the field distribution becomes quite uniform in the detection hot zone. The statistical analyses of field intensity at the hot zone and at the center plane of AgNP monolayer film are shown in (c) and (d), respectively. In particular, the standard deviation of field intensity at the hot zone is only about 10% of the peak value.

EXPERIMENTAL SECTION

Synthesis of Colloidal AgNPs and Preparation AgNP Films. Diethylene glycol (DEG) solution of silver colloidal nanoparticles (Ag colloids) was prepared by mixing 15 mL of poly(acrylic acid) (PAA)/DEG solution (0.81 g PAA + 15 mL DEG) with 3 mL of silver nitrate mixture (0.1 g $AgNO_3$ + 3 mL DEG) at 245 °C (the boiling point of DEG) and was maintained for 10 min. The octadecanethiolate-passivated AgNPs were synthesized by using a two-step, two-phase colloidal method.[28] In this step, an AgNP/DEG solution was transferred to toluene using tetraoctylammonium bromide (TOAB) as the transfer agent, and AgNPs were capped with octadecanethiolates in toluene. Specifically, 5 mL of AgNP/DEG solution was mixed with 10 mL of 100 mM TOAB/toluene solution, 10 mL of 100 mM octadecanethiolate/toluene solution, and 25 mL of toluene. The mixture was stirred vigorously for ~10 min and stood for 6 h. Then, we removed the bottom DEG solution. Finally, we utilized a centrifuge to purge the octadecanethiolate-passivated AgNP/toluene solution. Colloidal AgNPs exhibit many advantages to serve as plasmonic building blocks, such as well-controlled synthesis, size monodispersity, good shape control, facile surface functionalization, and excellent plasmonic properties in the visible light region. As for the large-scale self-assembly of plasmonic nanoparticle films, we have adopted a simple and efficient method for forming large-area (>1 cm^2), single- or multiple-layer AgNP films.[30] In comparison to a single-layer AnNP film, Janus nanoparticles[31] that simultaneously display two distinctly different surface properties are utilized to form multiple-layer AgNP films. Using this method, an arbitrary number of close-packed nanoparticle monolayers can be formed by using layer-by-layer assembly from a suspension of thiolate-passivated AgNPs, similar to the Langmuir–Blodgett technique.

Analytes in Spin-on-Glass (SOG). In this work, the SiO_2 layers were prepared from a diluted SOG solution (liquid form of methylsiloxane, IC1-200, Futurrex). The thickness of SiO_2 layer can be controlled by the spinning speed. To prepare a 5 nm thick SiO_2 layer, SOG was spun for 40 s at 5000 rpm and then dried at room temperature for a few minutes. To prepare the samples for Raman measurements, the analyte molecules were first dissolved in the spin-on-glass solution and then spun on under the same conditions. The analyte molecules used here do not have any chemical reaction with the SOG. The areal density of analytes can be estimated by the mass concentration of analytes in the SOG solution. The areal densities of analytes are estimated by the concentration of analytes and the thickness of SOG before drying. The volume contraction ratio (V_{dry}/V_{wet}) depends on the concentration of diluted SOG solution and can be experimentally determined.

Raman Measurements. Three different Raman systems were used, and all Raman measurements were performed at room temperature. In the Raman system I, the Raman spectra were acquired using a confocal Raman microscope. A 1 mW (before the microscope), 532 nm diode laser was used to excite the sample through a 100x objective (N.A. = 0.9, Olympus) with a laser spot diameter ~2 μm. The two-dimensional (2D) Raman mapping results were acquired on two independent systems (Raman systems II and III). The Ramon system II is a home-built confocal Raman microscope system. A 25–50 μW (after the microscope objective), 532 nm diode laser was used to excite the samples through a 100× objective (N.A. = 0.9, Olympus) with a laser spot diameter ~0.25 μm. The Raman system III is a

DOI: 10.1021/jacs.5b09111
J. Am. Chem. Soc. 2015, 137, 13698–13705

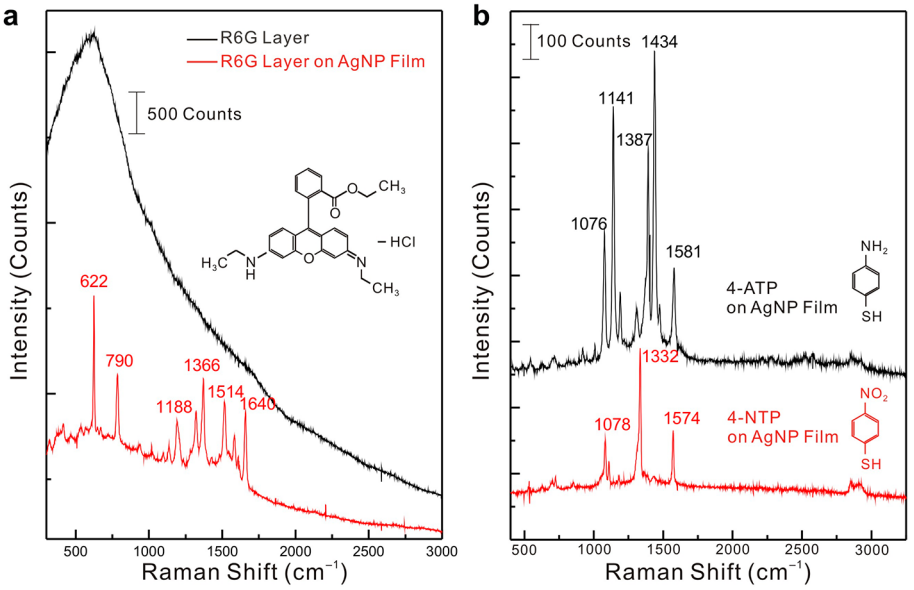

Figure 3. AgNP monolayer films as SERS substrates for three different analyte molecules. The areal densities are around 50000 molecules/μm^2. (a) Two Raman spectra obtained for a rhodamine 6G (R6G)/SOG layer on quartz (black) and a R6G/SOG layer on AgNP film (red), respectively. (b) Two Raman spectra obtained for a 4-aminothiophenol (4-ATP)/SOG layer on AgNP film (black) and a 4-nitrothiophenol (4-NTP)/SOG layer on AgNP film (red), respectively. The spectra were acquired by using the Raman System I.

commercial confocal Raman microscope system (LABRAM HR 800 UV, Horiba Jobin-Yvon). A 1 mW (before the microscope), 514 nm Ar-ion laser was used to excite the sample with a laser spot diameter ~0.7 μm.

Simulations. The finite-difference time-domain (FDTD) simulations were performed by using a commercial package (Lumerical, FDTD solutions v.7.5). The simulated structures of the nanoparticle monolayer film adopted the structure parameters measured by scanning electron microscopy. The in-plane structure (x–y plane) is a hexagonal close-packed array. The unit cell of investigated structure is simulated using periodic boundary conditions along the x and y axis, and perfectly matched layers along the propagation direction of the electromagnetic wave (z axis). The dielectric function of silver was adopted from the experimental data by Johnson and Christy.[32] The refractive index of the surrounding medium was assumed to be 1.5.[33] The simulation mesh with is 0.3 nm, and the periodic boundary condition is adopted.

RESULTS AND DISCUSSION

We have previously demonstrated that layer-by-layer assembled colloidal gold and silver nanoparticle films exhibit strong and tunable plasmonic response. The adopted self-assembly method for creating nanoparticle films is quite simple, robust, and scalable.[28,30] In this study, AgNPs are chosen as the building blocks of SERS substrates because of their superior plasmonic properties among all plasmonic metals. Figure 1a shows the field-emission scanning electron microscopy (FE-SEM) image of one monolayer (1 ML), close-packed AgNP superlattice film. The diffraction pattern via fast Fourier transform confirms the long-range ordering of AgNP superlattice.

Besides protecting the AgNPs from ambient-induced degradation and regulating the formation of hot-spot array, additional important advantage of thiolate ligands on the nanoparticle surface is that the collective plasmon resonance modes of close-packed AgNP films can be varied by changing the near-field coupling strength between adjacent nanoparticles. Using this approach, the plasmonic peak position can be tuned precisely by varying the carbon-chain length of alkanethiolate ligands and the resulting interparticle spacing.[28] This plasmonic coupling effect can be readily visualized by the purple and green colors displayed in the transmission and reflection photographs, respectively (Figure 1b). Additionally, the measured optical absorbance of 1 ML AgNP film confirms the plasmonic resonance at 500 nm (shown in Supporting Information Figure S1).

Figure 1c shows our experimental approach to control the distance between SERS substrate and analytes. The analytes were dissolved in SOG solution and then spin-coated on the 1 ML AgNP film. After drying/curing, ultrathin analyte/SOG glass layers can be prepared reproducibly using this method since the concentration of analytes is dilute enough that the viscosity of SOG is not significantly altered. For the demonstration shown in Figure 1, we utilize CV molecules as the analytes, which were embedded in a 5 nm thick SOG layer with an estimated areal density of about 5000 molecules/μm^2. In Figure 2, we show the FDTD simulation results that all of the analytes can be located in a controllable hot zone and with a uniform enhancement factor. Our method of introducing analytes is critical for quantitative SERS measurements because those analytes distribute homogeneously above the AgNP film within a precise spatial range for reproducible SERS detection.

Figure 1d shows the Raman spectra of a CV/SOG layer on an AgNP film, a bare AgNP film, and a bare CV/SOG layer, respectively. Althought the excitation wavelength of 532 nm is in the resonant absorption regime for CV molecules, the strong Raman signal of CV molecules can only be observed with the AgNP film. This result confirms the Raman enhancement via the plasmonic resonance of AgNP film (Supporting Information Figure S2 illustrates the srong dependendence on the excitation laser wavelength). In addition, to confirm that this enhancement effect is generally applicable, we have also tried different molecules, including rhodamine 6G (R6G), 4-nitrothiophenol (4-NTP) and 4-aminothiophenol (4-ATP), as shown in Figure 3. It is important to note that this Raman enhancement effect cannot be realized if the wavelength of

DOI: 10.1021/jacs.5b09111
J. Am. Chem. Soc. 2015, 137, 13698–13705

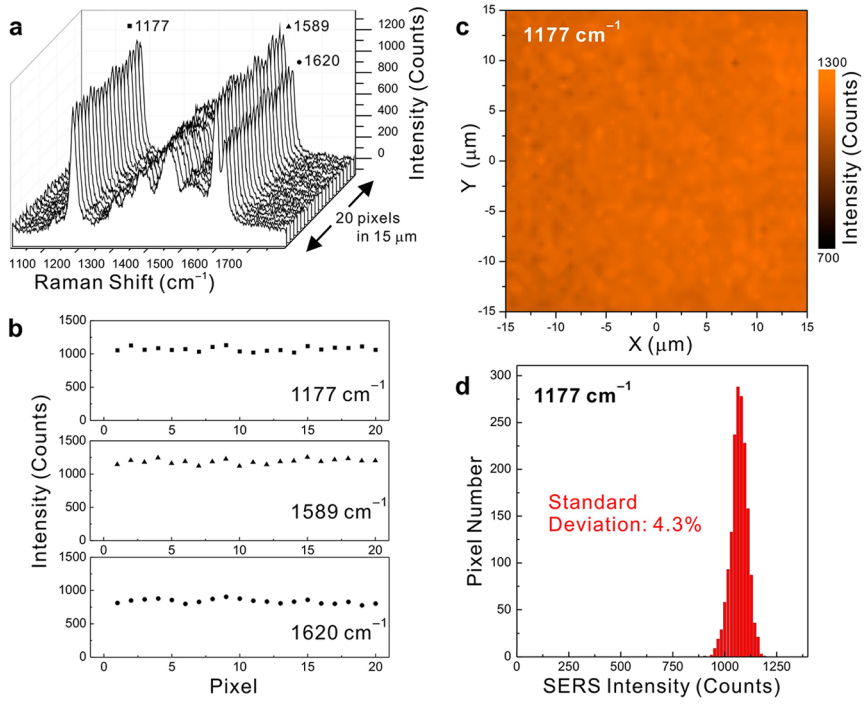

Figure 4. Uniformity of SERS substrate. (a) SERS spectra from a CV/SOG layer on top of a 1 ML AgNP film. The areal densities are around 5000 molecules/μm^2. The spectra were taken using the Raman System III and the integration time is 1 s. Spectra in the linescan was taken with a 0.75 μm step size. (b) Variation of SERS intensity at the specific Raman modes of 1177, 1589, and 1620 cm^{-1}, respectively. (c) Raster-scanning image showing the SERS intensity mapping (41 × 41 pixels) over a large area of 30 × 30 μm^2 at the Raman signal of 1177 cm^{-1}. (d) Standard deviation is only 4.3%.

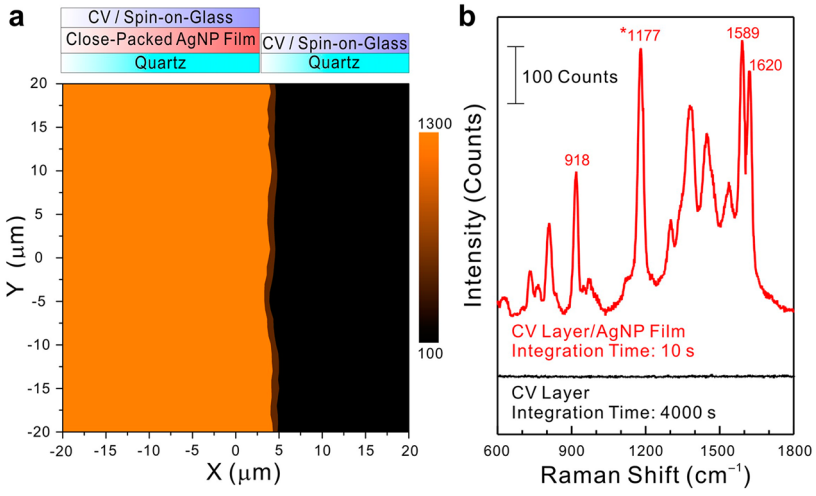

Figure 5. Enhancement factor of AgNP SERS substrate. (a) SERS mapping near an edge of an AgNP film. The spectra were acquired by using the Raman System II and the integration time is 1 s. The whole area is covered by a CV/SOG layer with an estimated molecule areal density of 5000/μm^2. (b) Two Raman spectra (vertically offset for clarity) were obtained from a 5000-molecules/μm^2 CV/SOG layer on AgNP film and a 500000-molecules/μm^2 CV/SOG layer on quartz, respectively. The enhancement factor can be estimated to be large than 1.2 × 10^7, which is derived by 300 (Raman intensity ratio at 1177 cm^{-1}) × 400 (integration time ratio) × 100 (areal density ratio).

excitation laser does not match with the plasmonic resonance peak (see Supporting Information Figure S2).

We found that the AgNP film exhibited an excellent Raman enhancement uniformity for SERS measurements. Figure 4 presents the Raman mapping results from a CV/SOG layer deposited on the whole imaged area. Figure 4a shows a Raman linescan with 20 spectra in 15 μm scanning distance and the intensities of some specific CV Raman peaks (i.e., 1177, 1589, and 1620 cm^{-1}) are displayed in Figure 4b. Figure 4c is a two-dimensional Raman mapping at the CV Raman peak of 1177 cm^{-1}. The scanning area is 900 μm^2 and the total number of imaging pixels are 1681 (41 × 41). As shown in Figure 4c, every pixel shows a uniform Raman peak intensity. The standard deviation is only 4.3% (Figure 4d), which is a record-low value at the ensemble measurement level.[13,23] It is worth pointing out that the detected region presented here was randomly selected, and consistent spatial uniformity can be found in the whole SERS substrate.

Uniform hot spot properties across the self-assembled nanoparticles film is an important prerequisite for achieving

DOI: 10.1021/jacs.5b09111
J. Am. Chem. Soc. 2015, 137, 13698−13705

spatial uniformity in SERS. Here, it is accomplished by the formation at highly regular thiolate-encapsulated AgNP superlattice. Another key requirement is the homogeneous distribution of analytes in the designated detection hot zone. The hottest sites on the close-packed AgNP film locate at the interparticle gap, where are spatially blocked by the alkanethiolates. According to our FDTD simulations shown in Figure 2, the mean field intensity in the designated detection hot zone above the AgNP film is about ten times smaller than that at the hottest sites, but the spatial uniformity is much better. Indeed, there is a trade-off between enhancement factor and spatial uniformity. The optimized detection geometry adopted in this study could provide both strong enhancement factor for single molecule detection and high spatial uniformity. The reported SERS enhancement factor in the literature is usually quite misleading since the SERS signal changes significantly across the SERS substrate. Owing to the uniform SERS signal across the SERS substrate, we could perform a reliable enhancement factor measurement. Figure 5a shows the Raman mapping result near the edge of a CV/SOG layer-covered AgNP film. The Raman mapping is clearly separated into two regions, revealing the uniform and large SERS enhancement originated from the AgNP film.

To precisely estimate the enhancement factor, we performed a control experiment (longer data acquisition time, as shown in Figure 5b) using the same Raman system and a sample with a higher concentration of CV in the SOG layer. The estimated enhancement factor is more than 1.2×10^7, which is sufficiently high for single-molecule measurements.[10] Also, Supporting Information Figure S3 shows another control experiment in which an additional SOG dielectric layer is introduced between the analytes and the SERS substrate. The results show that the uniformity is better but the enhancement factor is much lower because of the presence of the additional dielectric layer. Furthermore, according to the FDTD simulations (Figure 2), we estimated that the enhancement factor at the hottest sites on the AgNP film could be large than 10^9 because the field intensity is more than ten times stronger. This is consistent with the previous results reported for nanogaps formed by colloidal gold nanoparticles.[21] In Supporting Information Figure S4, we show that large SERS enhancement can also be observed by using the R6G molecules.

The absolute Raman scattering intensity depends on both instrumental factors (laser power, optical alignment, resolution of spectrometer, and sensitivity of detector, etc.) and other intrinsic properties (scattering cross sections of Raman modes and wavelength- or polarization-dependence on the excitation laser, and bonding configuration of molecules with the substrate, etc.). Therefore, utilizing the Raman intensity to determine the precise concentration of analytes is very difficult. Fortunately, using our SERS substrates, the Raman signal from the alkanethiolate ligands on AgNPs can be utilized as a stable internal calibration standard for quantitative SERS measurements. The Raman signals of analytes from different instruments are now accountable by normalizing them with respect to the SERS signal from the internal standard. In Figure 6a, the SERS intensity of CV molecules change proportionally with their areal density (50−5000 molecules/μm^2) in the 5 nm thick SOG layer, whereas the SERS intensity of alkanethiolates on the AgNP surface remains at the same level (original data sets are shown in Supporting Information Figure S5). Thus, we can define a normalized/calibrated CV SERS intensity by the ratio of SERS intensities from CV and alkanethiolate. Figure 6b shows that the normalized/calibrated SERS intensities of different CV/SOG layers exhibit a well-defined linear response (correlation coefficient $R > 0.999$) over a wide areal density range (5−5000 molecules/μm^2). Note that these data points are collected from two Raman measurement systems using different measurement conditions. According to our measurement results, this linear relationship can be used as a universal areal density ruler for analyte molecules, such that any analyte density can be quantitatively determined by the normalized (calibrated) analyte SERS signal.

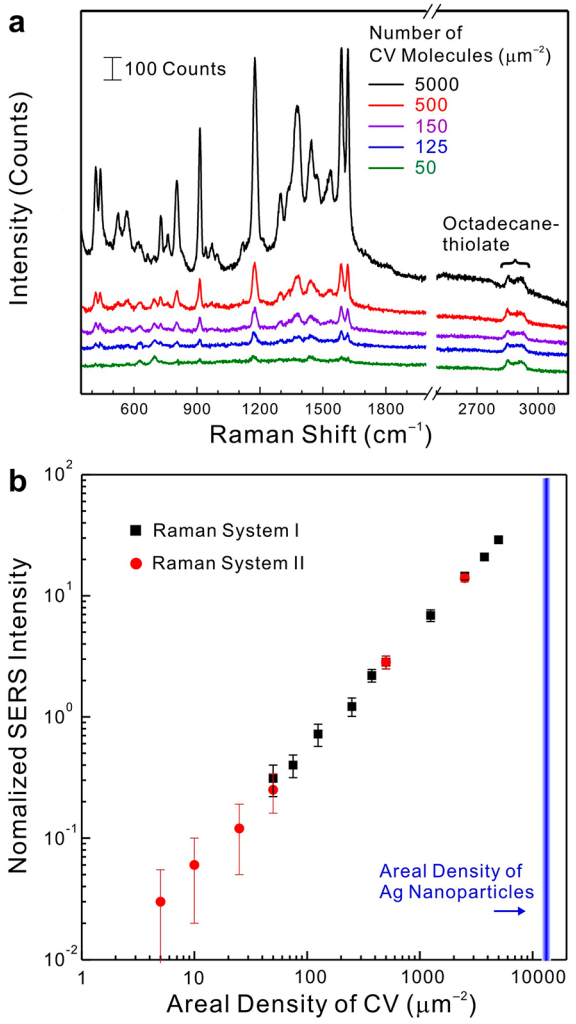

Figure 6. Quantitative SERS measurements. (a) CV-density-dependent SERS spectra (vertically offset for clarity). The spectra were acquired by using the Raman System I and the integration time is 10 s. (b) Normalized CV intensity at 1177 cm^{-1} as a function of CV molecules. The SERS signal of alkanethiolate ligands (octadecanethiolates) is utilized to calibrate and normalize the SERS signals obtained for CV molecules at different areal densities. The areal densities of CV molecules were varied from 5 to 5000 molecules/μm^2. These data are collected from two different Raman instruments. The black and red points are obtained by using the Raman Systems I and II (some representative Raman spectra are shown in Supporting Information Figure S5), respectively. The error-bar shows the standard deviation of SERS intensities at different sample locations. The error bars are larger at ultralow density levels because of the statistical nature of a Poisson distribution, where the error bars are proportional to $1/\sqrt{N}$ (N is the number of events).

It should be noted that the present approach of embedding analytes in an ultrathin spin-on-glass layer is for a proof-of-

DOI: 10.1021/jacs.5b09111
J. Am. Chem. Soc. 2015, 137, 13698−13705

concept experimental study of quantitative SERS. Using this method, we can achieve both strong Raman enhancement factor for single-molecule detection and high spatial uniformity across the SERS substrate. However, it might not be suitable for all analytes to be detected. For the general-purpose SERS applications (especially for the case that analytes are in liquid solutions), we still can use an ultrathin, analyte-free SOG layer on the alkanethiolate-regulated AgNP film (SERS substrate) to control the Raman enhancement factor and to achieve high spatial uniformity, whereas the analytes are dispersed in the nearby medium by using, for example, a microfluidic system.[14] To achieve evanescent detection near the SERS substrate, the total-internal-reflection (TIR) excitation technique[34,35] can be applied to perform TIR Raman spectroscopy.[36−38] Using this experimental technique, the ultrathin SOG layer with a properly functionalize surface allows for highly uniform SERS hot-zone and the evanescent excitation of TIR makes sure that only the analytes in close proximity to the SERS substrate are detected. One additional advantage is that the built-in internal SERS standard (thiolate ligands) in this quantitative SERS approach is not affected by the location of analytes (within the SOG layer or in the optical evanescent field).

CONCLUSION

Reliable, scalable, and tunable SERS substrates are developed for quantitative SERS measurements at the single-molecule level. This is achieved by the precise control of SERS enhancement factor and detection hot zone using ligand-regulated silver nanoparticle superlattices with a built-in internal standard. Several model molecules have been demonstrated in this study. We expect that the establishment of quantitative SERS technique for single-molecule detection will open up many exciting opportunities for both fundamental and applied research areas.

ASSOCIATED CONTENT

Supporting Information

The Supporting Information is available free of charge on the ACS Publications website at DOI: 10.1021/jacs.5b09111.

Plasmonic resonance of AgNP monolayer film (Figure S1), Raman experiments at different excitation laser wavelengths (Figure S2), a control experiment confirming that the Raman signal can be enhanced by avoiding anomalously hot detection sites on the SERS substrate (Figure S3), enhancement factor of AgNP SERS substrate via R6G molecules (Figure S4), and Raman measurement results at extremely low CV densities (Figure S5). (PDF)

AUTHOR INFORMATION

Corresponding Authors

*hungying@mx.nthu.edu.tw (H.Y.C.)
*gwo@phys.nthu.edu.tw (S.G.)

Notes

The authors declare no competing financial interest.

ACKNOWLEDGMENTS

We would like to acknowledge financial support from the Ministry of Science and Technology (MOST) in Taiwan through research grants MOST 104-2628-M-007-001 (S.G. and Y.M.C.), MOST 104-2112-M-007-020 (H.Y.C.), MOST 102-2218- E-007-012-MY3 (S.G.), and MOST 103-2633- M-007-001 (S.G.). We would also like to thank Prof. Nyan-Hwa Tai at National Tsing-Hua University for the access of a confocal Raman microscope system (Raman system III).

REFERENCES

(1) Fleischmann, M.; Hendra, P. J.; McQuillan, A. J. *Chem. Phys. Lett.* **1974**, *26*, 163−166.
(2) Jeanmaire, D. L.; Van Duyne, R. P. *J. Electroanal. Chem. Interfacial Electrochem.* **1977**, *84*, 1−20.
(3) Moskovits, M. *Rev. Mod. Phys.* **1985**, *57*, 783−826.
(4) Le Ru, E. C.; Etchegoin, P. G. *Principles of Surface-Enhanced Raman Spectroscopy and Related Plasmonic Effects*; Elsevier: Amsterdam, 2009.
(5) Nie, S.; Emory, S. R. *Science* **1997**, *275*, 1102−1106.
(6) Kneipp, K.; Wang, Y.; Kneipp, H.; Perelman, L. T.; Itzkan, I.; Dasari, R. R.; Feld, M. S. *Phys. Rev. Lett.* **1997**, *78*, 1667−1670.
(7) Le Ru, E. C.; Meyer, M.; Etchegoin, P. G. *J. Phys. Chem. B* **2006**, *110*, 1944−1948.
(8) Dieringer, J. A.; Lettan, L. B.; Scheidt, K. A.; Van Duyne, R. P. A *J. Am. Chem. Soc.* **2007**, *129*, 16249−16256.
(9) Kleinman, S. L.; Ringe, E.; Valley, N.; Wustholz, K. L.; Phillips, E.; Scheidt, K. A.; Schatz, G. C.; Van Duyne, R. P. *J. Am. Chem. Soc.* **2011**, *133*, 4115−4122.
(10) Le Ru, E. C.; Blackie, E.; Meyer, M.; Etchegoin, P. G. *J. Phys. Chem. C* **2007**, *111*, 13794−13803.
(11) Fang, Y.; Seong, N.-H.; Dlott, D. D. *Science* **2008**, *321*, 388−392.
(12) Kleinman, S. L.; Frontiera, R. R.; Henry, A.-I.; Dieringer, J. A.; Van Duyne, R. P. *Phys. Chem. Chem. Phys.* **2013**, *15*, 21−36.
(13) Bell, S. E. J.; Sirimuthu, N. M. S. *Chem. Soc. Rev.* **2008**, *37*, 1012−1024.
(14) März, A.; Ackermann, K. R.; Malsch, D.; Bocklitz, T.; Henkel, T.; Popp, J. *J. Biophotonics* **2009**, *2*, 232−242.
(15) Shen, W.; Lin, X.; Jiang, C.; Li, C.; Lin, H.; Huang, J.; Wang, S.; Liu, G.; Yan, X.; Zhong, Q.; Ren, B. *Angew. Chem., Int. Ed.* **2015**, *54*, 7308−7312.
(16) Freeman, R. G.; Grabar, K. C.; Allison, K. J.; Bright, R. M.; Davis, J. A.; Guthrie, A. P.; Hommer, M. B.; Jackson, M. A.; Smith, P. C.; Walter, D. G.; Natan, M. J. *Science* **1995**, *267*, 1629−1632.
(17) Jackson, J. B.; Halas, N. J. *Proc. Natl. Acad. Sci. U. S. A.* **2004**, *101*, 17930−17935.
(18) Wang, H.; Levin, C. S.; Halas, N. J. *J. Am. Chem. Soc.* **2005**, *127*, 14992−14993.
(19) Fan, M.; Brolo, A. G. *Phys. Chem. Chem. Phys.* **2009**, *11*, 7381−7389.
(20) Li, J. F.; Huang, Y. F.; Ding, Y.; Yang, Z. L.; Li, S. B.; Zhou, X. S.; Fan, F. R.; Zhang, W.; Zhou, Z. Y.; Wu, D. Y.; Ren, B.; Wang, Z. L.; Tian, Z. Q. *Nature* **2010**, *464*, 392−395.
(21) Lim, D.-K.; Jeon, K.-S.; Hwang, J.-H.; Kim, H.; Kwon, S.; Suh, Y. D.; Nam, J.-M. *Nat. Nanotechnol.* **2011**, *6*, 452−460.
(22) Banholzer, M. J.; Millstone, J. E.; Qin, L.; Mirkin, C. A. *Chem. Soc. Rev.* **2008**, *37*, 885−897.
(23) Ko, H.; Singamaneni, S.; Tsukruk, V. V. *Small* **2008**, *4*, 1576−1599.
(24) Camden, J. P.; Dieringer, J. A.; Zhao, J.; Van Duyne, R. P. *Acc. Chem. Res.* **2008**, *41*, 1653−1661.
(25) Lin, X.-M.; Cui, Y.; Xu, Y.-H.; Ren, B.; Tian, Z.-Q. *Anal. Bioanal. Chem.* **2009**, *394*, 1729−1745.
(26) Sharma, B.; Cardinal, M. F.; Kleinman, S. L.; Greeneltch, N. G.; Frontiera, R. R.; Blaber, M. G.; Schatz, G. C.; Van Duyne, R. P. *MRS Bull.* **2013**, *38*, 615−624.
(27) Lal, S.; Grady, N. K.; Goodrich, G. P.; Halas, N. J. *Nano Lett.* **2006**, *6*, 2338−2343.
(28) Chen, C.-F.; Tzeng, S.-D.; Chen, H.-Y.; Lin, K.-J.; Gwo, S. *J. Am. Chem. Soc.* **2008**, *130*, 824−826.
(29) Zhang, D.; Xie, Y.; Deb, S. K.; Davison, V. J.; Ben-Amotz, D. *Anal. Chem.* **2005**, *77*, 3563−3569.

DOI: 10.1021/jacs.5b09111
J. Am. Chem. Soc. 2015, 137, 13698−13705

(30) Lin, M.-H.; Chen, H.-Y.; Gwo, S. *J. Am. Chem. Soc.* **2010**, *132*, 11259−11263.
(31) de Gennes, P. G. *Rev. Mod. Phys.* **1992**, *64*, 645−648.
(32) Johnson, P. B.; Christy, R. W. *Phys. Rev. B* **1972**, *6*, 4370−4379.
(33) Underwood, S.; Mulvaney, P. *Langmuir* **1994**, *10*, 3427−3430.
(34) Sönnichsen, C.; Geier, S.; Hecker, N. E.; von Plessen, G.; Feldmann, J.; Ditlbacher; Lamprecht, B.; Krenn, J. R.; Aussenegg, F. R.; Chan, V. C.-H.; Spatz, J. P.; Möller, M. *Appl. Phys. Lett.* **2000**, *77*, 2949−2951.
(35) Yang, S.-C.; Kobori, H.; He, C.-L.; Lin, M.-H.; Chen, H.-Y.; Li, C.; Kanehara, M.; Teranishi, T.; Gwo, S. *Nano Lett.* **2010**, *10*, 632−637.
(36) Wood, D. A.; Bain, C. D. *Analyst* **2012**, *137*, 35−48.
(37) McKee, K. J.; Meyer, M. W.; Smith, E. A. *Anal. Chem.* **2012**, *84*, 4300−4306.
(38) Zhao, Q.; Lu, D.-F.; Liu, D.-L.; Chen, C.; Hu, D.-B.; Qii, Z.-M. *Acta Phys.-Chim. Sin.* **2014**, *30*, 1201−1207.

DOI: 10.1021/jacs.5b09111
J. Am. Chem. Soc. 2015, 137, 13698−13705